

# PHYSICAL REVIEW B

## CONDENSED MATTER AND MATERIALS PHYSICS

THIRD SERIES, VOLUME 62, NUMBER 15

15 OCTOBER 2000-I

### BRIEF REPORTS

*Brief Reports are accounts of completed research which, while meeting the usual Physical Review B standards of scientific quality, do not warrant regular articles. A Brief Report may be no longer than four printed pages and must be accompanied by an abstract. The same publication schedule as for regular articles is followed, and page proofs are sent to authors.*

#### Contrasting bonding behaviors of 3d transition metal atoms with graphite and C<sub>60</sub>

Antonis N. Andriotis,<sup>1,\*</sup> Madhu Menon,<sup>2,3,†</sup> and George E. Froudakis<sup>4</sup>

<sup>1</sup>*Institute of Electronic Structure and Laser, Foundation for Research and Technology-Hellas, P.O. Box 1527, 71110 Heraklio, Crete, Greece*

<sup>2</sup>*Department of Physics and Astronomy, University of Kentucky, Lexington, Kentucky 40506-0055*

<sup>3</sup>*Center for Computational Sciences, University of Kentucky, Lexington, Kentucky 40506-0045*

<sup>4</sup>*Department of Chemistry, University of Crete, P.O. Box 1470, Heraklio, Crete, Greece 71409*

(Received 26 January 2000)

The interactions of 3d transition metal atoms with graphite and C<sub>60</sub> molecule is investigated using tight-binding molecular-dynamics and *ab initio* methods. The results for vanadium and nickel confirm recent experimental deduction of the contrasting bonding behaviors between the early and the late 3d-transition metals in their interaction with graphite and C<sub>60</sub>. Furthermore, our results reveal the role of substrate relaxation and curvature in producing a striking dissimilarity in the bonding behaviors among transition metal atoms on graphite and C<sub>60</sub>.

The interaction of graphite and C<sub>60</sub> with the transition metal atoms (TMA's) has been the subject of intense research investigations due to the vast number of potential applications these systems may have in nanotechnology, materials research, and catalysis. These investigations (for comprehensive recent reviews see references<sup>1,2</sup>) have also been recently extended to include single wall carbon nanotubes<sup>3,4</sup> (SWCN's) since the TMA's have been found to play a dominant role in the production and other properties of the SWCN's.<sup>3,5</sup> The variety of the behavior found in the interaction between the TMA's with graphite is further enriched in the case of C<sub>60</sub> and the SWCN's as curvature and zone folding effects are additionally involved.<sup>4,6,7</sup> This results from strong hybridization strength between the carbon *p* and the TMA *d* orbitals as well as significant rehybridization process due to the curvature. The range of variation in the interaction appears to be more pronounced in the case of the C<sub>60</sub>-TMA system, where C<sub>60</sub> was found to possess a great ability to adapt itself to various environments, being able to act either as an electron donor or as an electron acceptor.

Experimental investigations of the interaction between the 3d-TMA's and the C<sub>60</sub> have indicated a different behavior of the early 3d-elements (Sc, Ti, V) when compared with those of the late 3d elements (Fe, Co, Ni).<sup>8</sup> Similar differentiation

was also observed in the case of bonding type and the binding sites on the same systems when experimental studies of C<sub>60</sub> with the TMA clusters were performed.<sup>8-11</sup> In particular, experimental measurements of small  $M_m(C_{60})_n^+$  clusters ( $M = \text{Sc, Ti, V}$ ), indicate no external *M* atoms and favor  $M_1[\eta^6-(C_{60})_2]$ , where  $\eta^6$  indicates that six ligand (carbon-ring) atoms are bonded to the metal (*M*) atom. These results led to the conclusion that the  $M(C_{60})_2$ ,  $M = \text{Sc, Ti, V}$  clusters take the form of a dumbbell and that the *M* atom is sandwiched between the six-membered rings of C<sub>60</sub> rather than the five-membered rings. On the other hand, in the  $M_m(C_{60})_n$ ,  $M = \text{Fe, Co, Ni}$  clusters, C<sub>60</sub> was found to react rather as an  $\eta^3$  than as an  $\eta^6$  or  $\eta^5$  ligand. In the case of  $\text{Ni}_2(C_{60})_2$ , sideways or end on binding to the Ni dimer seemed to be a possibility.<sup>9</sup>

Analogous comparative experimental information about the interaction behavior of the 3d-TMA's with graphite has not yet been reported, to the best of our knowledge. However, theoretical investigations using density-functional methods<sup>12</sup> and the complete neglect of differential overlap method<sup>13</sup> have shown a differentiation in the interaction properties of the early 3d elements as compared to those of the late 3d elements.<sup>12</sup> Neither group, however, has incorpo-

TABLE I. Summary of results for V on graphite and the  $C_{60}$  molecule. Positive values of charge transfer indicate *loss* of charge on V, while negative values indicate *gain* in charge on V. The values of the magnetic moment  $\mu$  are in Bohr magnetons ( $\mu_B$ ). The numbers in parentheses denote the number of times the given quantity is repeated. For  $V_2(C_{60})_2$  refer to Fig. 2.

Cluster	Bonding type	Charge transfer (e)	$\mu$ ( $\mu_B$ )	V-C bonds ( $\text{\AA}$ )
V- $C_{128}$ (V-graphite)	hole	-1.344	1.021	1.847, 1.992 2.004, 2.010
	atop	0.816	0.543	[2.062-2.103](6)
V- $C_{60}$	hole	-1.703	0.952	2.209 (6)
	atop	-0.975	0.991	1.799, 2.017 (2)
	bridge	-0.129	2.911	1.831, 1.841
V-( $C_{60}$ ) <sub>2</sub>	dumbbell	0.623	0.249	[2.145-2.168](12)
	bent	0.426	0.235	1.896(2), 2.123(2), 1.804
$V_2(C_{60})_2$ (T1)	shown in Fig. 2(a) [r(V-V)=1.782]	0.461(V <sup>top</sup> =V <sup>bottom</sup> )	0.028	1.852, 2.215 2.249, 2.023(2)
	(T2)	shown in Fig. 2(b)	0.659(V <sup>right</sup> ) 0.499(V <sup>left</sup> )	0.054 0.133
(T3)	shown in Fig. 2(c)	0.304(V <sup>right</sup> )	0.049	2.110(2), 1.911(2), 1.828
		1.942(V <sup>left</sup> )	0.030	2.000(2), 1.797
(T4)	shown in Fig. 2(d) [r(V-V)=2.099]	-0.293(V <sup>left</sup> )	0.927	2.083(2), 2.018(2), 2.010
		-0.580(V <sup>right</sup> )	0.828	2.030(2), 2.087(2), 1.978

rated optimization of atomic coordinates in their calculations and obtained conflicting bonding sites for the same TMA. Our recent preliminary works show the importance of including the effects of optimization and the role of curvature for bonding in the case of Ni.<sup>4,6</sup>

Interestingly, the experimental investigations of the magnetic behavior of V monolayers grown on Ag(100) have led to contradicting results with some experiments pointing to the presence of magnetic moments and others to the absence.<sup>14,15</sup> Magnetic behavior, however, was found in V clusters only freshly evaporated on graphite with the evidence being associated with the satellite structure observed in the V 3s x-ray photoemission spectra.<sup>15</sup> Subsequent experimental measurements have shown the V 3s line shape to be very sensitive to the V-graphite distance, throwing its origin into dispute.<sup>16</sup> Adding to the controversy is the high-spin state obtained for a single V adatom on graphite ( $4\mu_B$ ).<sup>12,16</sup>

In this paper, we present a first systematic theoretical study of the interaction of V atoms on graphite and  $C_{60}$  by considering all possible bonding sites while comparing these results with those for Ni in our earlier works with a view to interpret existing experimental data. Our calculations are performed using our tight-binding molecular-dynamics (TBMD) method<sup>4-7</sup> as well as accurate *ab initio* methods.<sup>22</sup> The details of our TBMD formulation can be found elsewhere (see for example, Refs. 7 and 17-19). The method makes use of Harrison's universal scheme<sup>20</sup> incorporating realistic distance dependence of the Slater-Koster type<sup>21</sup> parameters. The use of a minimal parameter basis set makes the scheme more transferable between differing environments. More importantly, the TBMD scheme allows us to employ fully symmetry unconstrained optimization for all geometries considered. The database for fitting the parameters is obtained from ex-

periment whenever available. This parametrization has been used with success to study  $Ni_m C_n$  clusters of arbitrary sizes and the interaction of Ni with graphite,  $C_{60}$ , and SWCN's.<sup>4-7</sup> The TBMD calculations are further complemented by accurate *ab initio* methods.<sup>22</sup> The *ab initio* calculations were performed using the GAUSSIAN 98 program package and includes density-functional theory calculations with the three-parameter hybrid functional of Becke using the Lee-Yang-Parr correlation functional.<sup>22</sup> The atomic basis set used is of double zeta quality and includes relativistic effects for heavy atoms.

In the present paper, the graphite is simulated by a portion of a graphene sheet consisting of 128 carbon atoms. This size was found to be sufficient for ensuring convergence of the results with the cluster size. Molecular-dynamics relaxation resulted in stable bonding for V on graphite at hole and atop sites. The adsorption of V was accompanied by a considerable distortion of the graphene sheet, especially for C atoms in the neighborhood of the V atom. The total energies for the fully relaxed geometries were obtained using *ab initio* calculations and show the ordering;  $E_{hole} < E_{atop}$  with the hole site being more stable by 0.50 eV. This is contrary to the findings of Duffy and Blackman,<sup>12</sup> and the discrepancy can be attributed to the neglect of relaxation effects in their calculations. We note that the same energetic ordering was also obtained by us for Ni adsorption on graphite.<sup>7</sup> As in the case of Ni on graphite, no stable bridge sites were found for V. At each adsorption site, the V atom exhibits a magnetic moment and there is appreciable charge transfer to or from the graphite atoms. The actual values of these quantities as well as the bond lengths between V and the neighboring C atoms are given in Table I. It should be noted, however, that our results do not support the high-spin states for V on graphite reported

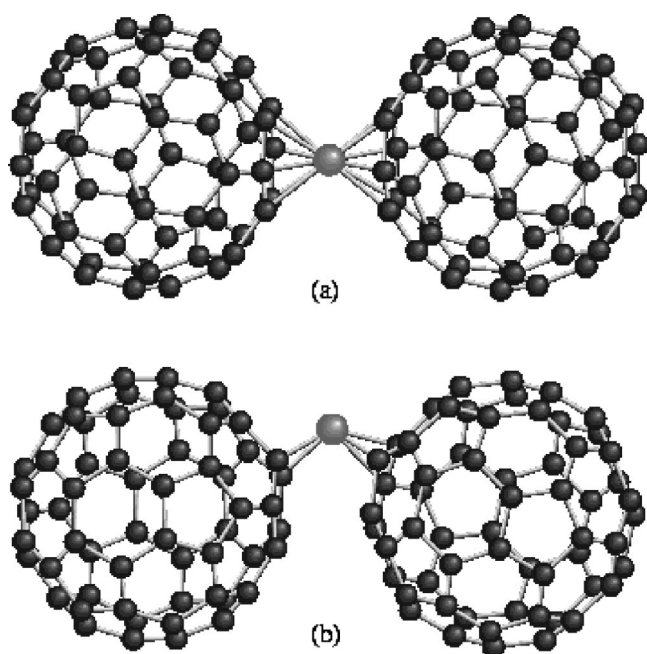


FIG. 1. Relaxed geometries for the  $V(C_{60})_2$  clusters.

recently.<sup>12,16</sup> This disagreement may be attributed to surface relaxation effects that have been completely omitted in Refs. 12 and 16.

For the  $VC_{60}$  cluster TBMD optimizations were carried out and the energetics of the fully relaxed structures were analyzed using *ab initio* methods to determine all the stable sites at which V can bind to  $C_{60}$ . We find that V binds at hole, atop, and bridge sites, while the total energies for these sites satisfy the relation  $E_{hole} < E_{atop} < E_{bridge}$ . The hole site was found to be more stable than atop and bridge sites by 0.37 eV and 0.95 eV, respectively. Note that for Ni, the hole site was found to be unstable, while the atop site was the most stable on  $C_{60}$ .<sup>6</sup> The only similarity here is that the bridge site now becomes stable for both V and Ni as a result of rehybridization due to the substrate curvature. It is also worth noting that our results for V on both graphite and  $C_{60}$  indicate the preference for V to act as an  $\eta^6$  ligand in con-

tradistinction with Ni, which acts as an  $\eta^2$  or  $\eta^3$  ligand,<sup>6</sup> in agreement with the experimental findings for both Ni and V interacting with  $C_{60}$ .<sup>8-11</sup> The V atom on the  $C_{60}$  exhibits a net charge and magnetic moment that depend on the adsorption site. The calculated net charge and magnetic moment of V as well as the bond lengths between the V and the nearest neighboring C atoms for the three adsorption sites (upon relaxation) are presented in Table I.

Vanadium is also found to bind two  $C_{60}$  molecules. Two of the most stable ground-state geometries for the  $V(C_{60})_2$  cluster are shown in Fig. 1. Among them the most stable one exhibits the dumbbell structure with both  $C_{60}$  molecules acting as  $\eta^6$  ligands [Fig. 1(a)]. It should be recalled that in the case of the  $Ni(C_{60})_2$  clusters, the most stable geometry also exhibited the dumbbell structure, but with one  $C_{60}$  molecule acting as  $\eta^2$  ligand and the other as  $\eta^3$  ligand.<sup>6</sup> These findings are in excellent agreement with the experimental results.<sup>8,10,11,2</sup> Table I contains the charge state, the magnetic moment of the V atoms, and the V-C bond lengths obtained for the  $V(C_{60})_2$  structures shown in Fig. 1.

All the stable geometries found for the  $V_2(C_{60})_2$  cluster are shown in Fig. 2. For the purposes of comparison we label them T1, T2, T3, and T4 and they correspond to Figs. 2(a), 2(b), 2(c) and 2(d), respectively. The T1 configuration is the most stable, with the energetics of the others in the order:  $E(T1) < E(T3) < E(T2) < E(T4)$ . The T1 structure has also been found to be the most stable configuration for the  $Ni_2(C_{60})_2$  cluster, with the connectivity via the formation of  $\eta^2$  and  $\eta^3$  ligands.<sup>6</sup> In the case of V, however, the connectivity is via the formation of  $\eta^3$  and  $\eta^4$  ligands [Fig. 2(a)]. Interestingly, the T1 structure has been deduced from the experiments of Kurikawa *et al.*<sup>10</sup> for  $Co_2(C_{60})_2$  clusters. More experimental works on the  $V_2(C_{60})_2$  clusters are needed for verifying our predictions.

Thus, a comparison of the results for V graphite and  $V-C_{60}$  demonstrates that the substrate-curvature effects can make qualitative differences in the relative stability of the various adsorption sites. Furthermore, qualitative differences between V (early 3d-TMA) and Ni (late 3d-TMA) are also evident in the study of the stable adsorption sites for these two elements on graphite and  $C_{60}$ .

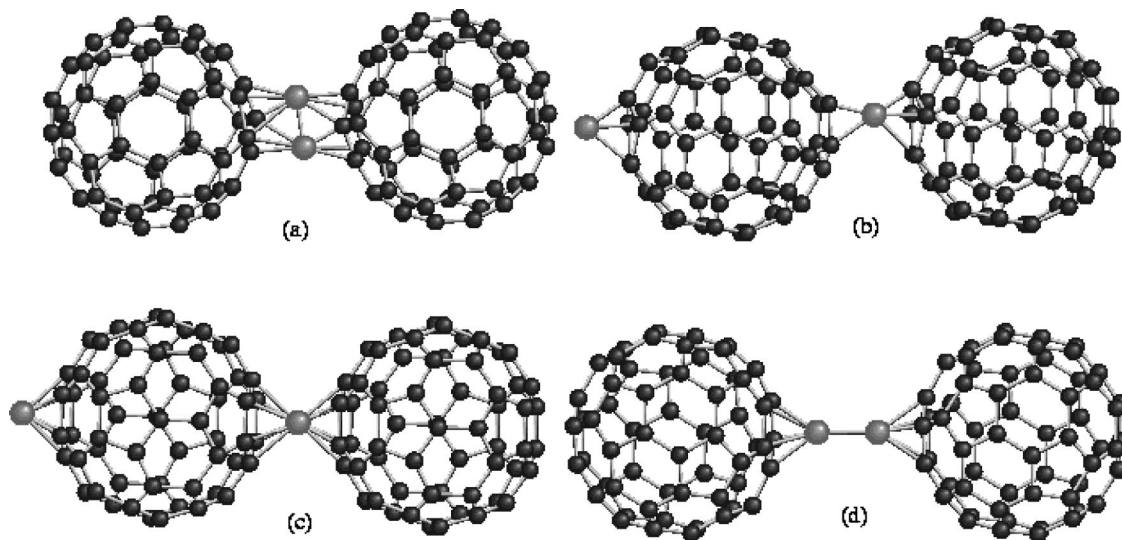


FIG. 2. Stable geometries for the  $V_2(C_{60})_2$  clusters.

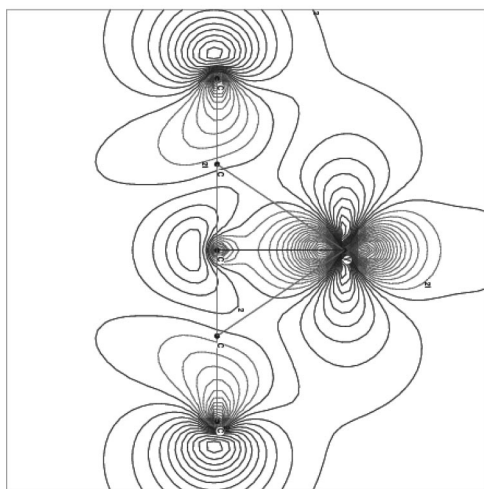


FIG. 3. Bonding HOMO's in the interaction of V with graphite at the hole site.

The qualitatively different behavior found in the case of V and Ni in their interactions with graphite and the  $C_{60}$  can be attributed mainly to the different occupancies of the adsorbate  $d$  orbitals. Another factor contributing to this is the variation of the hybridization strength between the adsorbate  $d$  orbitals and the  $p_z$  orbitals of graphite (the  $z$  axis is perpendicular to the surface). While the occupancy of the  $d$ -orbitals depends on the adsorbate atom and is affected by inter-atomic and intra-atomic charge-transfer effects, the hybridization strength depends on the point-group symmetry of the adsorption site (i.e.,  $C_{6v}$  for hole,  $C_{3v}$  for atop, and  $C_{2v}$  for bridge sites), the surface relaxation near the adsorbate, and the adsorbate-substrate distance. The presence of all these factors make a meaningful quantitative deduction of the contribution of each single factor to the interaction between a  $3d$  element and the graphite (or the  $C_{60}$ ) seem quite difficult. However, we can obtain an insight into the bonding behavior of Ni and V on graphite by studying the highest occupied molecular orbitals (HOMO's) using *ab initio* methods.

As an example, in Fig. 3 we show the HOMO's for V on a perfect graphite surface at the hole position. From these it

can be seen that for V at the hole site, the bonding molecular orbital (MO) is a perturbed  $d_{xz}$ . The bond at this site exhibits a weak covalent character. Similar analysis of Ni bonding at the hole site also reveals perturbed  $d_{xz}$  type but having a slightly stronger covalent character. We have also performed HOMO's analysis for Ni and V at the atop site and find the molecular orbitals for both to be of  $d_{3z^2-r^2}$  type. However, V bond exhibits strong covalent character, while the Ni bond exhibits ionic character. It should be noted that charge transfer, surface relaxation, and adsorbate-substrate distance, all influence the relative bond strengths between atop and hole sites. Furthermore, both surface relaxation, and the surface curvature rehybridizes the bonding MO's and results in a small covalent contribution in addition to the ionic bond between Ni and graphite.<sup>4</sup> It is, therefore, not surprising that atop site appears more stable than the hole site and vice versa, as the geometric configuration changes. Our disagreement with the results of Refs. 12 and 16 and may be attributed to the important contribution of surface relaxation effects that have been left out in those works.

Similar results obtained in studies in which the  $C_{60}$  is replaced by a SWCN lead us to believe that the differences found in the bonding between V and Ni on  $C_{60}$  (and SWCN) may also manifest as the differences in the contact resistances when these TMA's attach themselves to SWCN walls.<sup>23</sup>

We have, thus, demonstrated the important roles played by substrate relaxation, curvature of the substrate, occupancy of the  $d$  orbital of the adsorbate, and the point-group symmetry of the adsorption site in determining the relative stabilities of  $3d$  TMA at various adsorption sites on graphite and  $C_{60}$ . Furthermore, Ni and V were also found to exhibit substantial magnetic moments and undergo significant charge transfer processes that depend on the detailed configuration of their adsorption sites on both the graphite and the  $C_{60}$ .

The present work was supported through grants by NSF (OSR 98-62485, OSR 99-07463, MRSEC Program under award number DMR-9809686), DEPCoR (OSR 99-63231 and OSR 99-63232), the Semiconductor Research Corporation (SRC), and the University of Kentucky Center for Computational Sciences.

\*Email address: andriot@iesl.forth.gr

†Email address: super250@pop.uky.edu

<sup>1</sup>C. Binns, S.H. Baker, C. Denangeat, and J.C. Parlebas, Surf. Sci. Rep. **34**, 105 (1999).

<sup>2</sup>P. Mathur, I.J. Mavunkal, and S.B. Umbarkar, J. Cluster Sci. **9**, 393 (1998).

<sup>3</sup>L. Grigorian, G.U. Sumanasekera, A.L. Loper, S.L. Fang, J.L. Allen, and P.C. Eklund, Phys. Rev. B **60**, R11 309 (1999).

<sup>4</sup>A.N. Andriotis and M. Menon, Chem. Phys. Lett. **320**, 425 (2000).

<sup>5</sup>A.N. Andriotis, M. Menon, and G.E. Frudakis, Phys. Rev. Lett. **85**, 3193 (2000).

<sup>6</sup>A.N. Andriotis and M. Menon, Phys. Rev. B, **60**, 4521 (1999).

<sup>7</sup>A.N. Andriotis, M. Menon, G.E. Froudakis, and J.E. Lowther, Chem. Phys. Lett. **301**, 503 (1999).

<sup>8</sup>S. Nagao, T. Kurikawa, K. Miyajima, A. Nakajima, and K. Kaya, J. Chem. Phys., **102**, 4495 (1998).

<sup>9</sup>E.K. Parks, K.P. Kerns, S.J. Riley, and B.J. Winter, Phys. Rev. B **59**, 13 431 (1999).

<sup>10</sup>T. Kurikawa, S. Nagao, K. Miyajima, A. Nakajima, and K. Kaya, J. Chem. Phys. **102**, 1743 (1998).

<sup>11</sup>A. Nakajima, S. Nagao, H. Takeda, T. Kurikawa, and K. Kaya, J. Chem. Phys. **107**, 6491 (1997).

<sup>12</sup>D.M. Duffy and J.A. Blackman, Phys. Rev. B **58**, 7443 (1998).

<sup>13</sup>T. Montero, Z. Benzo, A. Sierraalta, and F. Ruetter, in *Surfaces, Vacuum, and their Applications*, edited by I. Hernandez-Calderon and R. Asomoza (AIP, Woodbury, NY, 1994).

<sup>14</sup>P. Kruger, M. Taguchi, J.C. Parlebas, and A. Kotani, Phys. Rev. B **55**, 16 466 (1997).

<sup>15</sup>C. Binns, H.S. Derbyshire, S.C. Bayliss, and C. Norris, Phys. Rev. B **45**, 460 (1992).

<sup>16</sup>P. Kruger, J.C. Parlebas, and A. Kotani, Phys. Rev. B **59**, 15 093 (1999).

<sup>17</sup>A.N. Andriotis and M. Menon, Phys. Rev. B **57**, 10 069 (1998).

- <sup>18</sup>N.N. Lathiotakis, A.N. Andriotis, M. Menon, and J. Connolly, *J. Chem. Phys.* **104**, 992 (1996).
- <sup>19</sup>A.N. Andriotis, M. Menon, G. Froudakis, Z. Fthenakis, and J.E. Lowther, *Chem. Phys. Lett.* **292**, 487 (1998).
- <sup>20</sup>W. Harrison, in *Electronic Structure and Properties of Solids* (W. H. Freeman, San Francisco, 1980).
- <sup>21</sup>J.C. Slater and G.F. Koster, *Phys. Rev.* **94**, 1498 (1954).
- <sup>22</sup>Gaussian 98, Revision A.6, M.J. Frisch *et al.* (Gaussian, Inc., Pittsburgh, 1998).
- <sup>23</sup>A.N. Andriotis, M. Menon, and G. Froudakis, *Appl. Phys. Lett.* **76**, 3890 (2000).